



Article

Value of SUV_{max} for the Prediction of Bone Invasion in Oral Squamous Cell Carcinoma

Stephanie A. Stalder ^{1,2}, Paul Schumann ^{2,3}, Martin Lanzer ^{2,3}, Martin W. Hüllner ^{2,4} ,
Niels J. Rupp ^{2,5}, Martina A. Broglie ^{1,2} and Grégoire B. Morand ^{1,2,*} 

¹ Department of Otorhinolaryngology - Head and Neck Surgery, University Hospital Zurich, 8091 Zurich, Switzerland; stephstalder@gmx.ch (S.A.S.); martina.broglie@usz.ch (M.A.B.)

² Faculty of Medicine, University of Zurich, 8006 Zurich, Switzerland

³ Department of Cranio-Maxillo-Facial and Oral Surgery, University Hospital Zurich, 8091 Zurich, Switzerland; paul.schumann@usz.ch (P.S.); martin.lanzer@usz.ch (M.L.)

⁴ Department of Nuclear Medicine, University Hospital Zurich, 8091 Zurich, Switzerland; martin.huellner@usz.ch

⁵ Department of Pathology and Molecular Pathology, University Hospital Zurich, 8091 Zurich, Switzerland; niels.rupp@usz.ch

* Correspondence: gregoire.morand@usz.ch; Tel.: +41-44-255-58-50; Fax: +41-44-255-45-56

Received: 21 December 2019; Accepted: 31 January 2020; Published: 2 February 2020



Abstract: In advanced oral squamous cell carcinoma (OSCC), accurate planning of surgical resection and reconstruction are crucial for outcome and postoperative function. For OSCC close to the maxilla or mandible, prediction of bone invasion is necessary. The aim of this study was to examine whether metabolic tumor imaging obtained by fluorodeoxyglucose positron emission tomography (FDG-PET) could enhance preoperative predictability of bone invasion. We performed an analysis of 84 treatment-naïve OSCCs arising from gum (upper and lower), hard palate, floor of mouth, and retromolar trigone treated at the University Hospital Zurich, Switzerland, who underwent wide local excision with free flap reconstruction between 04/2010 and 09/2018 and with available preoperative FDG-PET. Prediction of bone invasion by metabolic tumor imaging such as maximum standardized uptake value (SUV_{max}) was examined. On definitive histopathology, bone invasion was present in 47 of 84 cases (56%). The probability of bone infiltration increased with a higher pretherapeutic SUV_{max} in an almost linear manner. A pretherapeutic SUV_{max} of primary tumor below 9.5 ruled out bone invasion preoperatively with a high specificity (97.6%). The risk of bone invasion was 53.6% and 71.4% for patients with SUV_{max} between 9.5–14.5 and above 14.5, respectively. Patients with bone invasion had worse distant metastasis-free survival compared to patients without bone invasion (log-rank test, $p = 0.032$). In conclusion, metabolic tumor imaging using FDG-PET could be used to rule out bone invasion in oral cancer patients and may serve in treatment planning.

Keywords: carcinoma; squamous cell; positron emission tomography; fluorodeoxyglucose F18; bone; tumor hypoxia

1. Introduction

Oral squamous cell carcinoma (OSCC) is an aggressive malignancy characterized by local invasiveness and high propensity to lymph node metastases [1]. OSCC is the sixth most common cancer worldwide and the most common site of malignancy in the head and neck [2]. Risk factors for OSCC include exposure to extrinsic carcinogens such as tobacco, alcohol, and betel nut [1,2]. The incidence of OSCC varies among geographical regions accordingly, with a high incidence in Melanesia, South Central Asia, Australia, and Europe [3]. The unchanging survival in patients with

OSCC underscores the need for better prognostic tools, as recently reported in the 8th edition of American Joint Committee on Cancer staging system [4].

OSCC is primarily amenable to surgery and requires wide local excision with macroscopical margins of usually at least 1.0 cm. In advanced cases, wide local excision leads to a substantial defect, which has to be reconstructed with a local or free flap [5].

If the tumor is close to the bone, but without bone invasion, it may be resected together with the periosteum. In select cases, a marginal mandibulectomy may be required as well. Reconstruction with a fascio-cutaneous or musculocutaneous soft tissue flap is then sufficient [2].

If the tumor has invaded the bone, a segmental mandibulectomy is often required. This requires a reconstruction using an osteo(myo)cutaneous free flap. Accurate preoperative assessment of bone invasion is hence an important prerequisite for reconstruction planning and patient consent [2].

While clinicians have traditionally relied on physical examination, including triple endoscopy, some have examined the accuracy of cross-sectional imaging such as computed tomography (CT) and/or magnetic resonance imaging (MRI) for bone invasion [6–10]. It turned out, however, that these modalities have limited diagnostic accuracy [10].

Recent studies suggest that metabolic tumor imaging with 18-fluorodeoxyglucose positron emission tomography (FDG-PET) could be useful for estimating the aggressiveness of a particular tumor [11–13]. Here, the most commonly used metabolic parameter is the maximum standardized uptake value (SUV_{max}).

Whether metabolic tumor imaging could add additional information for the prediction of bone invasion has not been investigated yet. Therefore, the goal of our study was to examine if FDG uptake could increase the predictability of bone invasion in OSCC.

2. Results

2.1. Patient and Tumor Characteristics

A total of 84 treatment-naïve patients with curative intent suffering from advanced OSCC from the upper and lower gum, retromolar trigone, floor of mouth, and hard palate with available pretherapeutic PET/CT or PET/MRI were included in this study (Table 1). The mean age at diagnosis was 67.3 (SD 11.0) years. There was a clear male predominance with 52 (61.9%) male and 32 (38.1%) female patients. Seventy-four (88.1%) had squamous cell carcinomas close to/with invasion of the mandible, and 10 patients (11.9%) close to/with invasion of the maxilla. Most patients (63.1%) had pT4 tumors while 33.3% and 3.6% of patients had pT1-pT2 and pT3 tumors, respectively. Nodal status was positive in 43 patients (51.2%), of which 17 (20.2%) were staged with pN1, 22 (26.2%) with pN2a-pN2b, and 4 (4.8%) with pN2c-pN3 categories.

The median pretherapeutic SUV_{max} was 14.10 (IQR 10.63–17.5) for the whole cohort. The median follow-up time for all patients was 20 months (IQR 9.25–36.25). A total of 46 patients (54.8%) were treated with adjuvant radio(chemo)therapy (Table 1).

Table 1. Patient Demographics and Clinical Characteristics.

Variable		All Patients No. of Patients = 84	Bone Invasion No. of Patients = 47	No Bone Invasion No. of Patients = 37	<i>p</i> Value ¹ B vs. nB
Age	Mean (SD)	67.3 (11.0)	69.3 (11.5)	64.7 (9.9)	0.055
Gender					
Male	No. (%)	52 (61.9%)	26 (55.3%)	26 (70.3%)	0.182
Female	No. (%)	32 (38.1%)	21 (44.7%)	11 (29.7%)	
Smoking	Yes (%)	43 (51.2%)	21 (44.7%)	22 (59.5%)	0.195
	No (%)	41 (48.8%)	26 (55.3%)	15 (40.5%)	
Alcohol consumption	Yes (%)	42 (50.0%)	19 (40.4%)	23 (62.2%)	0.128
	No (%)	42 (50.0%)	28 (59.6%)	14 (37.8%)	

Table 1. Cont.

Variable		All Patients No. of Patients = 84	Bone Invasion No. of Patients = 47	No Bone Invasion No. of Patients = 37	<i>p</i> Value ¹ B vs. nB
<i>cT-classification</i>					
T1-T2	No. (%)	22 (26.2%)	8 (17%)	14 (37.8%)	0.007
T3	No. (%)	5 (6.0%)	0	5 (13.5%)	
T4	No. (%)	57 (67.8%)	39 (83%)	18 (48.7%)	
<i>pT-classification</i>					
T1-T2	No. (%)	28 (33.3%)	0	27 (73%)	<0.001 *
T3	No. (%)	3 (3.6%)	0	3 (8.1%)	
T4	No. (%)	53 (63.1%)	47 (100%)	7 (18.9%)	
<i>pN-classification</i>					
N0	No. (%)	41 (48.8%)	18 (38.3%)	23 (62.2%)	0.023
N1	No. (%)	17 (20.2%)	8 (17%)	9 (24.3%)	
N2a-b	No. (%)	22 (26.2%)	18 (38.3%)	4 (10.8%)	
N2c-N3	No. (%)	4 (4.8%)	3 (6.4%)	1 (2.7%)	
<i>FDG-PET</i>					
SUV _{max} primary tumor	Median (IQR)	14.1 (10.6–17.5)	15.9 (11.1–18.9)	13.0 (8.1–16.0)	0.015 *

¹ T-Test for normally distributed variables. Mann–Whitney U Test for non-normally distributed variables, 2-sided Pearson chi-squared test for categorical variables. SUV_{max}: maximum standardized uptake value. *p*-value for null hypothesis; * statistically significant.

2.2. Patients with Bone Invasion Had Higher SUV_{max} of Primary Tumor

As depicted in Table 1, there were 47 patients with bone invasion and 37 without bone invasion. Comparisons between the two groups showed a trend towards older age in patients with bone invasion. As expected, there were significantly more patients classified as pT4 in the bone invasion group (chi-squared test, $p < 0.001$). The SUV_{max} of the primary tumor was significantly higher in the bone invasion group (Mann–Whitney U test, $p = 0.015$) (Figure 1).

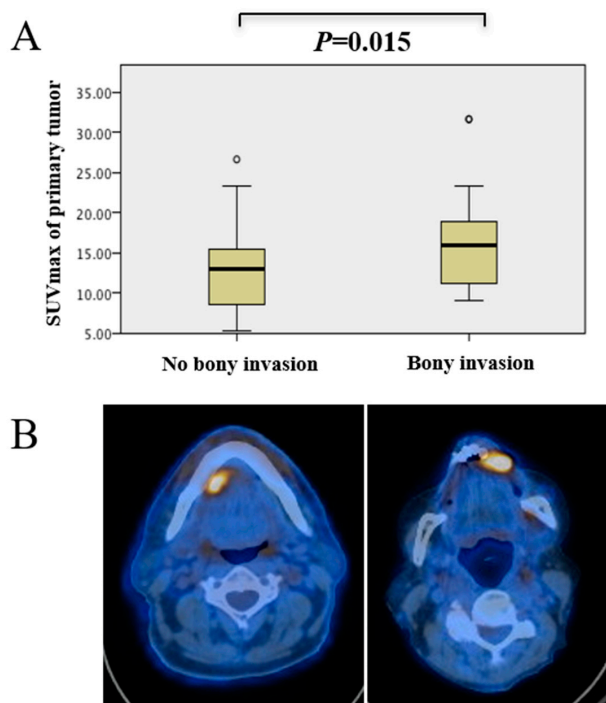


Figure 1. (A) Correlation between maximum standardized uptake value (SUV_{max}) of primary tumor and bone invasion. Oral squamous cell carcinoma (OSCC) with bone invasion showed a significantly higher SUV_{max} (Mann–Whitney U Test, $p = 0.015$). (B) Representative axial fused FDG-PET/CT images showing, on the left, a tumor with a low SUV_{max} (7.3). Histopathological analysis showed no bone invasion. On the right, the SUV_{max} was 21.8, and the tumor showed bone invasion.

2.3. Prediction of Mandibular Infiltration Using Clinical Examination, Computed Tomography (CT), and Magnetic Resonance Imaging (MRI)

The different modalities were compared against each other with regard to sensitivity and specificity for predicting bone invasion. Bone invasion assessed by definitive histopathological analysis was used as the gold standard. As shown in Table 2, clinical examination had limited sensitivity and specificity. CT had a poor sensitivity but a rather good specificity, meaning that a positive CT finding was very likely to predict bone invasion. MRI had a poorer diagnostic accuracy than CT for bone invasion.

Table 2. Comparative table of prediction of bone invasion compared to histopathological standard.

Variable	Histopathological Examination		
	TP	FP	Sensitivity
<i>Clinical examination</i>	40	19	67.8%
	FN	TN	Specificity
	7	18	72.0%
<i>Computed tomography (CT)</i>	TP	FP	Sensitivity
	13	1	72.2%
	FN	TN	Specificity
	5	11	91.6%
<i>Magnetic resonance imaging (MRI)</i>	TP	FP	Sensitivity
	28	6	73.3%
	FN	TN	Specificity
	8	19	76.0%
<i>SUV_{max} primary tumor < 9.5</i>	TP	FP	Sensitivity
	41	22	97.6%
	FN	TN	Specificity
	1	10	31.2%

TP: true positive. FP: false positive. FN: false negative. TN: true negative.

2.4. Prediction of Bone Invasion Using Metabolic Tumor Imaging

Various cutoff values for FDG uptake parameters were tested. Using receiver operating characteristic (ROC) curves, the best potential cutoff value for the pretherapeutic SUV_{max} of primary tumor was determined to be 9.5 (Figure 2; area under the curve (AUC) 66.5% (95% CI 53.9%–79.1%), $p = 0.015$). The risk for bone invasion was also evaluated in ordinal fashion. For patients with pretherapeutic SUV_{max} < 9.5, the risk for mandibular invasion was very low with 9.1%. It was 53.6% for patients with SUV_{max} between 9.5 and 14.5, while patients with a strong metabolically active primary (SUV_{max} > 14.5) had a very high risk (71.4%) for bone invasion. The risk for bone invasion increased with a higher pretherapeutic SUV_{max} in an almost linear manner, as depicted in Figure 3.

2.5. Enhanced Diagnostic Accuracy Using Metabolic Imaging

We integrated the metabolic imaging parameter SUV_{max} of primary tumor (with a cutoff value of 9.5) and calculated the sensitivity and the specificity for bone invasion. The sensitivity and specificity for metabolic tumor imaging were 97.6% and 31.2%, respectively.

In summary, computed tomography had a good specificity, while metabolic tumor imaging demonstrated a high sensitivity with a remarkably low number of false negatives (Table 2).

2.6. Survival Outcomes

We performed Kaplan–Meier analysis to examine relative survival according to bone invasion. Local recurrence-free survival (Figure 4, Panel A, log-rank, $p = 0.855$) and regional recurrence-free survival (Figure 4, Panel B, log-rank, $p = 0.536$) were similar for both groups. Patients with bone

invasion showed a worse distant metastasis-free survival (Figure 4, Panel C, log-rank, $p = 0.032$). Disease-specific survival was similar among the two groups (Figure 4, Panel D, log-rank, $p = 0.144$).

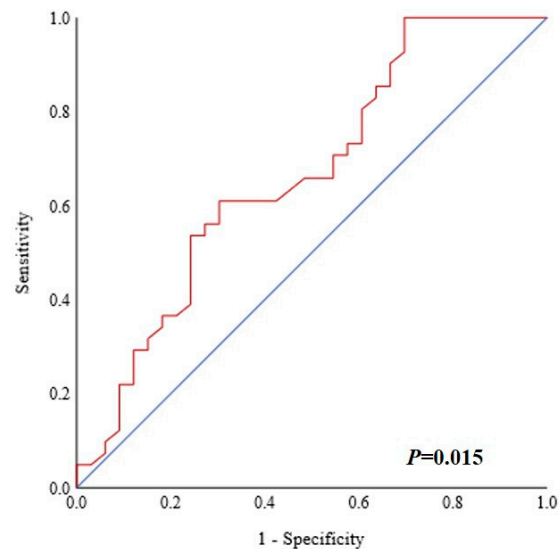


Figure 2. Receiver operating characteristic (ROC) curve showing the maximum standardized uptake value (SUV_{max}) and bone invasion. The best cutoff was determined to be 9.5. The area under the curve (AUC) was 66.5% (95% CI 53.9%–79.1%) ($p = 0.015$).

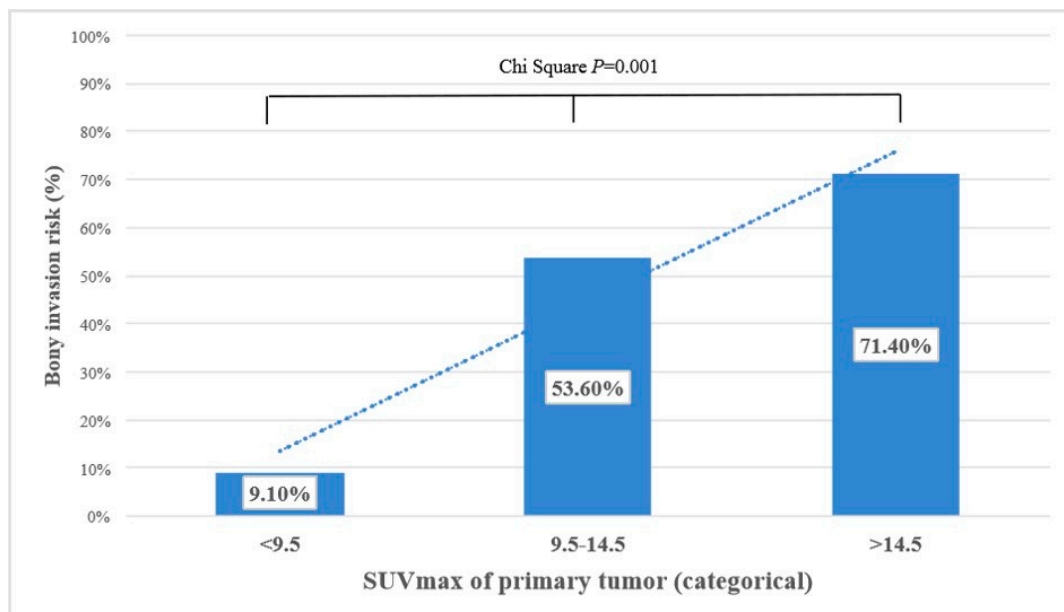


Figure 3. Categorical representation of maximum standardized uptake value (SUV_{max}) and bone invasion risk. Oral squamous cell carcinoma (OSCC) with low SUV_{max} had a very low risk for bone invasion, while the risk increased in an almost linear manner with increasing SUV_{max} (Pearson chi-squared test, $p = 0.001$).

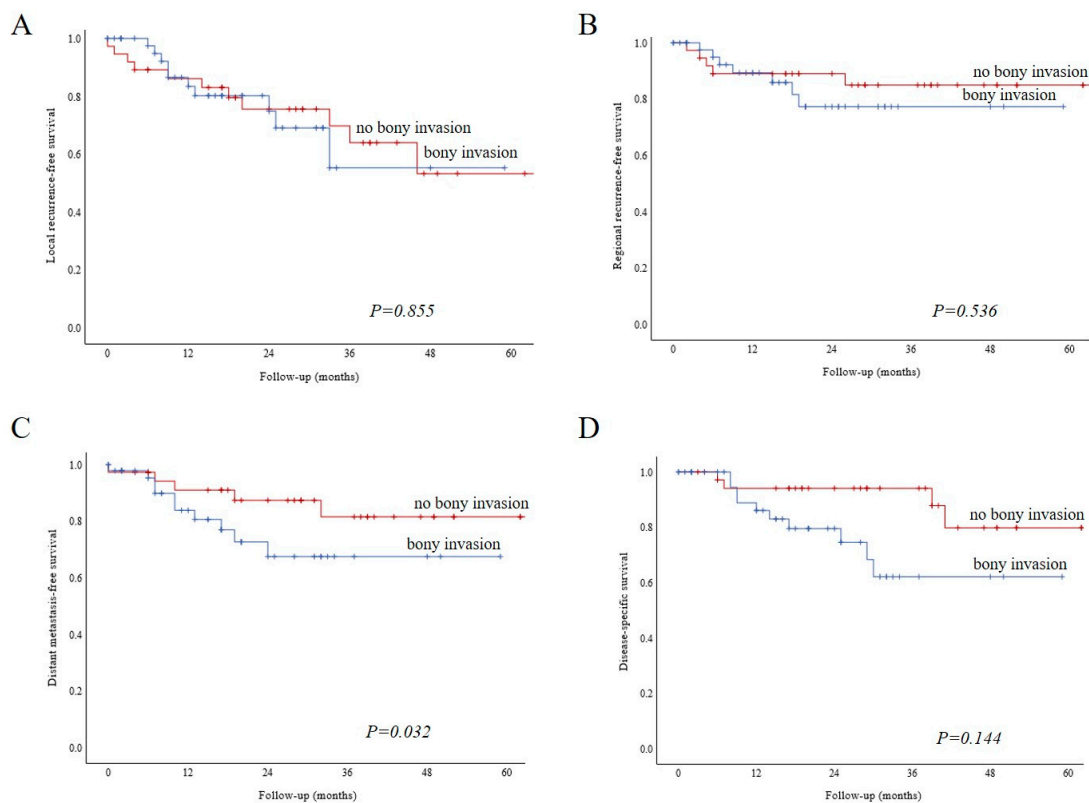


Figure 4. Kaplan–Meier analysis showing relative survival according to bone invasion. Local recurrence-free survival (A, log-rank, $p = 0.855$) and regional recurrence-free survival (B, log-rank $p = 0.536$) were similar for both groups. Patients with bone invasion had a worse distant metastasis-free survival. (C, Log-rank, $p = 0.032$). Disease-specific survival was similar among the two groups (D, log-rank, $p = 0.144$).

3. Discussion

This retrospective study evaluates the predictability of bone invasion by FDG-PET parameters of OSCC in a cohort of 84 patients. Primary tumor $SUV_{max} > 14.5$ showed a high probability for bone invasion, while the risk for bone invasion was low for primaries with $SUV_{max} < 9.5$. This study showed that considering the SUV_{max} of the primary tumor could increase the diagnostic accuracy for prediction of bone invasion by OSCC. Using such metabolic tumor imaging, the sensitivity of preoperative imaging could be considerably increased, mainly by reducing the number of false negatives. Practically, our findings imply that bone invasion can be largely ruled out if SUV_{max} of the primary OSCC tumor is < 9.5 with a sensitivity of 97.6%. Such a finding has a direct clinical applicability for treatment planning, considering complexity and complication rate for bone flaps compared to soft tissue flaps. Bone flaps require significant planning time for presurgical 3D planning for optimal bone and dental rehabilitation. They also have a higher failure rate than fascio- or musculocutaneous flaps [14].

Previous studies have examined the diagnostic accuracy of several imaging modalities for the prediction of bone invasion [6,7,9,10]. A metaanalysis by Qiao et al. reported the diagnostic accuracy of eight different diagnostic modalities. They showed a similar pooled accuracy of the examined modalities with heterogeneous and inconsistent data from each examined study. Regarding CT and MRI, their study found similar values for sensitivity and specificity as reported in our study [10], with a slightly better diagnostic accuracy for MRI than in our study. Qiao et al. did not report the diagnostic accuracy of the clinical examination and/or triple endoscopy. The latter is, however, quite difficult in clinical practice and not reliable enough. In our study, it was inferior to both CT and MRI.

When comparing CT and MRI, the latter seems to be more vulnerable for misinterpretation, owing to metal-related artifacts, while the former is more dependent on tumor origin and dentate status.

CT, however, showed a quite good specificity. Therefore, in case of positive bone invasion on CT, the latter is very likely to confirm on histopathological analysis. MRI had a rather poor diagnostic accuracy for bone invasion in our study.

For metabolic tumor imaging, an SUV_{max} of primary tumor <9.5 had a very high sensitivity, that is, allowing one to rule out the presence of bone invasion. This can be used nicely in complement to the CT findings.

FDG-PET seems to be slightly better than cross-sectional imaging alone, while a recent study by Sekine et al. showed that there is no overall difference between PET/CT and PET/MR in the detection of bone invasion [15]. False-positive findings of bone marrow invasion are reported for FDG-PET. They were significantly higher in edentulous patients than in dentate patients [7]. One possible explanation is the presence of periodontitis, which leads to dental loss and higher FDG uptake due to inflammatory process [7]. This is generally a drawback of FDG-PET, which has a very good sensitivity but is prone to false-positive results due to, e.g., inflammation [16].

The role of the teeth in conditioning the bone invasion of the mandible and maxilla remains controversial. Edentulous patients are thought by some to be more prone to bone infiltration than dentate patients, as teeth represent a relative barrier against tumor infiltration, and tooth loss leads to reduction of the height and occlusal surface of the mandible [15]. Some authors suggest, however, that the tumor can gain access to the dentate mandible through the periodontal membrane and invade more easily. Finally, others found that bone invasion occurs mainly at the point of junction of the attached gingival and reflected mucosa of the alveolar bone in both dentate and edentulous patients [2,16].

As shown in previous reports, SUV_{max} seems to be the metabolic parameter showing the highest reliability among all metabolic parameters [12,13]. It represents the single voxel with the most intense FDG uptake of a lesion and can be assessed easily and with high reproducibility. Hence, the SUV_{max} is a parameter that is used in daily clinical practice in every PET center worldwide.

In previous studies, we described that metabolic tumor imaging can be used as a surrogate to determine tumor aggressiveness [12,13]. Aggressive tumors undergo many genotypic and phenotypic changes through epithelial-mesenchymal transition (EMT) and cancer stem cells (CSC) enrichment to acquire invasive and metastatic properties [17]. Among others, these changes results in the expression of CD44, which allows cells to invade more deeply the surrounding tissue and enhances the glycolytic phenotype of cancer cells that are exposed to hypoxia [18]. The metabolic changes in hypoxic tumors induce tumor cells to increasingly metabolize glucose through glycolysis rather than the oxygen-dependent Krebs cycle (Warburg effect) [19]. An overall enhanced glucose consumption is observed in cancer cells with an increase of glucose transporter 1 (GLUT1) expression [20,21]. The glucose uptake of the tumor increases, which can be quantified using the SUV_{max} of FDG-PET. As a result, the SUV_{max} may be used as a surrogate marker for tumor aggressiveness, because it is positively correlated with tumor hypoxia.

Our study used different PET scanners with partly different reconstruction methods. However, the SUV_{max} is a standardized and comparably stable parameter. Our study did not stratify tumors by subsites in the oral cavity, although we did exclude OSCC tumors without any close anatomical relationship with the bone (oral tongue, buccal mucosa). It is known that tumors arising in the upper and lower gum or floor of the mouth are more prone to bone invasion than, e.g., tongue tumors [15]. It would have been exceedingly difficult, if not impossible, to create a truly comparable cohort of patients with or without bone invasion. Instead, we chose to include all OSCCs close to the bone with free flap reconstruction, thus avoiding selection bias. Further, we did not analyze the association between bone turnover markers and metabolic tumor imaging parameters. Some studies indeed reported the possibility of measuring bone turnover markers (such as bone sialoprotein) to increase the predictability of bone metastases [22,23]. It would have been very interesting to see if similar observations could be made for OSCC, bone invasion, and metabolic tumor imaging.

In conclusion, we showed that metabolic tumor imaging could be a useful clinical tool for ruling out bone infiltration in OSCC, simply by considering the SUV_{max} . This can easily be accomplished in clinical routine.

4. Materials and Methods

4.1. Study Population

After Ethics Review Board approval by the *Kantonale Ethikkommission Zürich* (protocol number 2016-01799, including amendment of 14 December 2018), all patients treated for squamous cell carcinoma of the oral cavity (OSCC) between 1 April 2010 and 1 September 2018, at the Department of Otorhinolaryngology – Head and Neck Surgery and the Department of Maxillofacial Surgery of the Zurich University Hospital, Switzerland, were retrospectively assessed. Study methods were carried out in accordance with the relevant guidelines and regulations. Informed consent of all enrolled patients was obtained. All patients with advanced oral cancer undergoing wide local excision and neck dissection and reconstruction were included. Only OSCC arising from the floor of mouth, upper and lower gum, hard palate, and retromolar trigone were included. Primary tumors from the lip, oral tongue, and the buccal mucosa were excluded. Primary study outcomes were predictors of bone invasion to the mandible or the maxilla. To determine predictors of bone invasion, clinical, radiological, and metabolic tumor imaging factors were assessed. Histopathological proof of bone invasion served as the gold standard. Secondary study outcomes were local-recurrence-free, regional-recurrence-free, distant-metastasis-free, and disease-specific survival.

Inclusion criteria were available pretherapeutic FDG-PET/CT or FDG-PET/MR images and treatment-naïve patients with curative intent. Patients treated surgically after induction chemotherapy were excluded.

All patients were staged according to the *Union Internationale Contre le Cancer* (UICC), TNM staging for head and neck cancer, 7th edition, 2010. We chose to use the 7th edition and not restage all patients with the UICC 8th edition, as the clinical decisions (imaging, surgery, adjuvant treatment) were based on the 7th edition of the TNM staging, which was in use at the time of treatment in all subjects [24]. After full medical history, physical examination, triple endoscopy with biopsy, and imaging with FDG-PET were performed. All patients were presented and discussed at the local multidisciplinary tumor board. Frozen sections were used intraoperatively to assure free mucosal and soft tissue margins of the surgical resection specimen. All patients had negative margins upon final pathology (R0).

Detailed data on age, gender, smoking, drinking habits, clinical and pathological tumor stage, bone invasion, local and regional recurrence, distant metastasis, disease-specific survival, and overall survival were obtained. Smoking was defined as a current daily consumption of cigars or cigarettes. Alcohol consumption was defined as a daily intake of more than 20 g of ethanol for at least five days a week. The study cohort was then divided into two groups according to the presence or absence of bone invasion defined by histopathology.

4.2. FDG-PET/CT or -/MR Image Acquisition

Patients were injected with a standardized dose of 3.5 MBq of 18-fluorodeoxyglucose (FDG) per kilogram body weight after fasting for at least four hours. All patients had a blood glucose level below 12 mmol/L before imaging. Patients were instructed to remain in a lying or recumbent position and silent for 50–60 min to minimize muscular FDG uptake in the period between FDG injection and image acquisition. Patients were also kept warm prior to tracer injection and throughout the uptake period to diminish FDG accumulation in brown adipose tissue. All patients received either iodinated or gadolinium-based contrast medium. An integrated Discovery VCT PET/CT system (GE Healthcare, Waukesha, WI, USA), a Discovery PET/CT 690 (GE Healthcare), or a hybrid PET/MRI system (Signa PET/MR, GE Healthcare) was used for image acquisition.

4.3. Image Assessment

Selected parameters of tumor FDG metabolism were recorded under supervision of a dually board-certified nuclear physician and radiologist and included SUV_{max} of the primary tumor. SUV_{max} was calculated automatically using a standard formula (maximum activity in region of interest \div (injected dose \times body weight)). A correct referencing of FDG uptake was ensured through side-by-side reading of the corresponding CT or MR images of the tumor in the axial, coronal, and sagittal plane. Borders of regions of interest (ROI) were set by manual adjustment to exclude adjacent physiologic FDG-avid structures. A written report by a dually board-certified nuclear medicine physician/radiologist was available for all FDG-PET/CT or -/MR images.

4.4. Statistical Analysis

For continuous variables, distribution was evaluated for normality according to Gauss' theorem. For normally distributed variables (age), mean and standard deviations are given, and comparison among study groups was done using the t-test. For non-normally distributed variables (smoking, SUV_{max} primary tumor, follow-up time), median and interquartile range (IQR) are given. To compare distribution among samples, the nonparametric Mann–Whitney U test was used for two samples. Binary variables were associated in contingency tables using the two-tailed Pearson chi-squared test. Bone invasion was defined by histopathology. The sensitivity and specificity of clinical examination, morphological cross-sectional imaging (MR and CT) and combined modality with FDG-PET metabolic parameter were calculated according to Bayes' theorem. Receiver operating characteristic (ROC) curves were used to select the best cutoff value for SUV_{max} to predict high risk for bone invasion with the 95% confidence interval provided (95% CI). Survival curves were built according to Kaplan–Meier, and the log-rank test was used to compare factors. A p -value lower than 0.05 was considered to indicate statistical significance. Statistical analyses were performed using SPSS® 25.0.0.1 software (IBM®, Armonk, NY, USA).

5. Conclusions

In this retrospective study, we showed that metabolic tumor imaging could be a useful clinical tool for ruling out bone invasion in OSCC, simply by considering the SUV_{max} . This can easily be accomplished in clinical routine due to good accessibility in many facilities. Treatment planning could be more concise because of good predictability of whether bone invasion is present or not considering SUV_{max} of the primary. Future studies shall examine the performance of SUV_{max} in a prospective setting as a help for treatment and reconstruction planning.

Author Contributions: Study idea by G.B.M. Patients search by S.A.S. S.A.S. extracted the patients' related data, built the figures, and wrote the first draft of the manuscript under G.B.M.'s supervision. G.B.M. performed statistical analysis. Interpretation of data, manuscript editing, and review were done by P.S., M.L., M.W.H., N.J.R., and M.A.B. All authors participated substantially in the study and approved the final version of the manuscript.

Acknowledgments: S.A.S. would like to thank her family, B.G., and her loved ones for their support.

Conflicts of Interest: The authors declare no conflict of interest as defined by Biology or other interests that might be perceived to influence the results and/or discussion reported in this paper.

References

1. Morand, G.B.; Broglie, M.A. *Therapie des Mundhöhlenkarzinoms: Tumorkontrolle und Funktionalität*; MedEdition: Hirzel, Switzerland, 2019.
2. Shah, J.P.; Gil, Z. Current concepts in management of oral cancer—surgery. *Oral Oncol.* **2009**, *45*, 394–401. [[CrossRef](#)]
3. Bray, F.; Ferlay, J.; Soerjomataram, I.; Siegel, R.L.; Torre, L.A.; Jemal, A. Global cancer statistics 2018: GLOBOCAN estimates of incidence and mortality worldwide for 36 cancers in 185 countries. *CA Cancer J. Clin.* **2018**, *68*, 394–424. [[CrossRef](#)]

4. Mascitti, M.; Rubini, C.; De Michele, F.; Balercia, P.; Girotto, R.; Troiano, G.; Lo Muzio, L.; Santarelli, A. American Joint Committee on Cancer staging system 7th edition versus 8th edition: Any improvement for patients with squamous cell carcinoma of the tongue? *Oral Surg. Oral Med. Oral Pathol. Oral Radiol.* **2018**, *126*, 415–423. [[CrossRef](#)]
5. Morand, G.B.; Broglie, M.A.; Schüler-Garcia, H.I. Radiotherapie versus Chirurgie für Kopf-Hals-Tumoren (Mundhöhle, Oropharynx, Larynx, Hypopharynx). *Trill. Krebsmed.* **2018**, *27*, 426–434.
6. Gu, D.H.; Yoon, D.Y.; Park, C.H.; Chang, S.K.; Lim, K.J.; Seo, Y.L.; Yun, E.J.; Choi, C.S.; Bae, S.H. CT, MR, (18)F-FDG PET/CT, and their combined use for the assessment of mandibular invasion by squamous cell carcinomas of the oral cavity. *Acta Radiol.* **2010**, *51*, 1111–1119. [[CrossRef](#)] [[PubMed](#)]
7. Abd El-Hafez, Y.G.; Chen, C.C.; Ng, S.H.; Lin, C.Y.; Wang, H.M.; Chan, S.C.; Chen, I.H.; Huan, S.F.; Kang, C.J.; Lee, L.Y.; et al. Comparison of PET/CT and MRI for the detection of bone marrow invasion in patients with squamous cell carcinoma of the oral cavity. *Oral Oncol.* **2011**, *47*, 288–295. [[CrossRef](#)] [[PubMed](#)]
8. Huang, S.H.; Chien, C.Y.; Lin, W.C.; Fang, F.M.; Wang, P.W.; Lui, C.C.; Huang, Y.C.; Hung, B.T.; Tu, M.C.; Chang, C.C. A comparative study of fused FDG PET/MRI, PET/CT, MRI, and CT imaging for assessing surrounding tissue invasion of advanced buccal squamous cell carcinoma. *Clin. Nuclear Med.* **2011**, *36*, 518–525. [[CrossRef](#)]
9. Pentenero, M.; Cistaro, A.; Brusa, M.; Ferraris, M.M.; Pezzuto, C.; Carnino, R.; Colombini, E.; Valentini, M.C.; Giovannella, L.; Spriano, G.; et al. Accuracy of 18F-FDG-PET/CT for staging of oral squamous cell carcinoma. *Head Neck* **2008**, *30*, 1488–1496. [[CrossRef](#)]
10. Qiao, X.; Liu, W.; Cao, Y.; Miao, C.; Yang, W.; Su, N.; Ye, L.; Li, L.; Li, C. Performance of different imaging techniques in the diagnosis of head and neck cancer mandibular invasion: A systematic review and meta-analysis. *Oral Oncol.* **2018**, *86*, 150–164. [[CrossRef](#)]
11. Liao, C.T.; Chang, J.T.; Wang, H.M.; Ng, S.H.; Hsueh, C.; Lee, L.Y.; Lin, C.H.; Chen, I.H.; Huang, S.F.; Cheng, A.J.; et al. Pretreatment primary tumor SUVmax measured by FDG-PET and pathologic tumor depth predict for poor outcomes in patients with oral cavity squamous cell carcinoma and pathologically positive lymph nodes. *Int. J. Radiat. Oncol. Biol. Phys.* **2009**, *73*, 764–771. [[CrossRef](#)]
12. Morand, G.B.; Vital, D.G.; Kudura, K.; Werner, J.; Stoeckli, S.J.; Huber, G.F.; Huellner, M.W. Maximum Standardized Uptake Value (SUVmax) of Primary Tumor Predicts Occult Neck Metastasis in Oral Cancer. *Sci. Rep.* **2018**, *8*, 11817. [[CrossRef](#)] [[PubMed](#)]
13. Werner, J.; Huellner, M.W.; Rupp, N.J.; Huber, A.M.; Broglie, M.A.; Huber, G.F.; Morand, G.B. Predictive Value of Pretherapeutic Maximum Standardized Uptake Value (Suvmax) In Laryngeal and Hypopharyngeal Cancer. *Sci. Rep.* **2019**, *9*, 8972. [[CrossRef](#)] [[PubMed](#)]
14. Zhou, W.; Zhang, W.B.; Yu, Y.; Wang, Y.; Mao, C.; Guo, C.B.; Yu, G.Y.; Peng, X. Risk factors for free flap failure: A retrospective analysis of 881 free flaps for head and neck defect reconstruction. *Int. J. Oral Maxillofac. Surg.* **2017**, *46*, 941–945. [[CrossRef](#)] [[PubMed](#)]
15. Sekine, T.; Barbosa, F.G.; Delso, G.; Burger, I.A.; Stolzmann, P.; Ter Voert, E.E.; Huber, G.F.; Kollias, S.S.; von Schulthess, G.K.; Veit-Haibach, P.; et al. Local resectability assessment of head and neck cancer: Positron emission tomography/MRI versus positron emission tomography/CT. *Head Neck* **2017**, *39*, 1550–1558. [[CrossRef](#)]
16. Brown, J.S.; Lowe, D.; Kalavrezos, N.; D’Souza, J.; Magennis, P.; Woolgar, J. Patterns of invasion and routes of tumor entry into the mandible by oral squamous cell carcinoma. *Head Neck* **2002**, *24*, 370–383. [[CrossRef](#)]
17. da Silva, S.D.; Morand, G.B.; Alobaid, F.A.; Hier, M.P.; Mlynarek, A.M.; Alaoui-Jamali, M.A.; Kowalski, L.P. Epithelial-mesenchymal transition (EMT) markers have prognostic impact in multiple primary oral squamous cell carcinoma. *Clin. exp. Metastasis* **2015**, *32*, 55–63. [[CrossRef](#)]
18. Morand, G.B.; Ikenberg, K.; Vital, D.G.; Cardona, I.; Moch, H.; Stoeckli, S.J.; Huber, G.F. Preoperative assessment of CD44-mediated depth of invasion as predictor of occult metastases in early oral squamous cell carcinoma. *Head Neck* **2019**, *41*, 950–958. [[CrossRef](#)]
19. Ngo, D.C.; Ververis, K.; Tortorella, S.M.; Karagiannis, T.C. Introduction to the molecular basis of cancer metabolism and the Warburg effect. *Mol. Biol. Rep.* **2015**, *42*, 819–823. [[CrossRef](#)]
20. Baschnagel, A.M.; Wobb, J.L.; Dilworth, J.T.; Williams, L.; Eskandari, M.; Wu, D.; Pruetz, B.L.; Wilson, G.D. The association of (18)F-FDG PET and glucose metabolism biomarkers GLUT1 and HK2 in p16 positive and negative head and neck squamous cell carcinomas. *Radiother. Oncol. J. Eur. Soc. Ther. Radiol. Oncol.* **2015**, *117*, 118–124. [[CrossRef](#)]

21. Tian, M.; Zhang, H.; Nakasone, Y.; Mogi, K.; Endo, K. Expression of Glut-1 and Glut-3 in untreated oral squamous cell carcinoma compared with FDG accumulation in a PET study. *Eur. J. Nucl. Med. Mol. Imaging* **2004**, *31*, 5–12. [[CrossRef](#)]
22. Uccello, M.; Malaguarnera, G.; Vacante, M.; Motta, M. Serum bone sialoprotein levels and bone metastases. *J. Cancer Res. Ther.* **2011**, *7*, 115–119. [[CrossRef](#)] [[PubMed](#)]
23. Ferreira, A.; Alho, I.; Casimiro, S.; Costa, L. Bone remodeling markers and bone metastases: From cancer research to clinical implications. *BoneKEy Rep.* **2015**, *4*, 668. [[CrossRef](#)] [[PubMed](#)]
24. Edge, S.B.; Compton, C.C. The American Joint Committee on Cancer: The 7th edition of the AJCC cancer staging manual and the future of TNM. *Ann. Surg. Oncol.* **2010**, *17*, 1471–1474. [[CrossRef](#)] [[PubMed](#)]



© 2020 by the authors. Licensee MDPI, Basel, Switzerland. This article is an open access article distributed under the terms and conditions of the Creative Commons Attribution (CC BY) license (<http://creativecommons.org/licenses/by/4.0/>).